NRL Memorandum Report 1784

AN/FPQ-6 Radar Antenna Gain Determination by Pattern Integration Techniques

DEAN D. HOWARD

Tracking Branch
Radar Division

June 23, 1967

NAVAL RESEARCH LABORATORY
Washington, D.C.

TABLE OF CONTENTS

ABSTRACT

The acceptance test gain determination for the 29 foot diameter Cassegrainian antenna of the AN/FPQ-6 radar was performed by antenna pattern integration techniques. This approach was used because of time limitations and difficulties of setting up an accurate boresight range for conventional gain comparison with a gain standard. By pattern integration of both the antenna and the feed patterns, the effective loss of near-in sidelobes and the spillover around the Cassegrainian sub-reflector could be determined separately with good accuracy. This approach gives considerable information on several characteristics of the antenna which led, in part, to changes for improving antenna performance. The less significant losses were estimated. The resultant gain determined by this technique averaged at 51.1-db over the band. This was confirmed at a later evaluation program where direct measurement gave an average gain of 51.2-db over the band.

PROBLEM STATUS

This is an interim report; work on the problem is continuing.

AUTHORIZATION

NRL Problem RO2-24
Project No. A05-535-208/652-1/F099-0502

AN/FPQ-6 RADAR ANTENNA GAIN DETERMINATION BY PATTERN INTEGRATION TECHNIQUES

INTRODUCTION

The AN/FPQ-6, Fig. 1, and AN/TPQ-18 (essentially identical but transportable version of the AN/FPQ-6) are precision monopulse instrumentation radars used on the NASA and Tri-Service Missile ranges. The initial radar was purchased on a very short procurement cycle of 13 months without prototype development; and factory acceptance testing was greatly limited by time and availability of special equipment to measure the performance of a state-of-the-art radar. One major problem was measurement of the gain of the antenna, specified at 51-db. The antenna uses a five horn monopulse Cassegrainian feed and 29-foot diameter solid surface paraboloidal reflector. The sub-reflector of the Cassegrainian feed is a convex hyperboloid 30 inches in diameter on adjustable mounts.

The acceptance test procedures called for measurement of antenna gain by the conventional direct comparison with a standard gain antenna. This presented a problem because the most accurately calibrated standard antennas are limited to the order of 17-db gain. At the long boresight tower distances required for a 51-db antenna, because of the near zone, the low elevation angle and broad beam of the standard horn results in severe multipath problems. The standard horn signal, in addition to multipath changes as a function of height, varied severely with time limiting measurement accuracy to about ± 2-db. Consequently, the possibility of determining multipath lobes to solve for direct signal energy was rejected as inadequate.

Several other techniques of measurement were considered. These include use of a higher gain secondary standard antenna, measurement of the total loss through the round-trip loop to a tracked sphere, and use of various absolute power level measurements. None of these techniques were found to be practical because of either time, expense, or possibility of excessive cumulative error.

A meeting of Naval Research Laboratory, Radio Corporation of America, and Air Force personnel was held to discuss the antenna gain measurement problem. The Navy was the Tri-Service procurement agency for the AN/FPQ-6 radar and the Air Force was the recipient of the initial models. NRL proposed to determine antenna gain by pattern integration techniques. This method offered acceptable accuracy with a minimum of expense. It also provided information on several other characteristics of the antenna in addition to the value of gain. The NRL integration technique was agreed upon and RCA provided the necessary patterns and other data.

ANTENNA GAIN DETERMINATION

The integration method proposed by NRL determines energy loss in the near-in sidelobes separately from the far-out sidelobes which represent spillover loss. This approach is used because the significant near-in sidelobes are well defined in the antenna patterns while the far-out sidelobes, being broad and low level, are difficult to measure accurately because of distortion by main beam reflections from buildings and other objects. In addition, the value of loss in the far-out sidelobes is strongly dependent on assumptions that must be made on lobe shape in the two dimensional region between the major antenna axes. Therefore, the integration is performed in two parts where the first step is the integration of the main lobe and the near-in sidelobes which result from the diffraction pattern of the parabola. This gives a basic gain figure exclusive of all other losses. The second step is the integration of feed patterns to determine the spillover loss which causes the major far-out sidelobes.

Other losses are small, being in the order of only a few tenths of a decibel, and typical values are assumed for these losses since even a large percentage error in these values is insignificant. However, the patterns are carefully examined to assure that none of the normally small losses have become large because of design problems or antenna damage.

The method chosen for pattern integration is the most conservative of two methods described below. Since three dimensional pattern plots (two angles plus amplitude) are not practical to obtain in the short time available for

acceptance testing, it is necessary to use the conventional single patterns. These are only infinitesimal slices through the two dimensional (azimuth and elevation) region; therefore, 45° patterns were obtained, in addition to azimuth and elevation patterns, to provide as much information as is practical within the time limitation. In the area between the single plane patterns there are regions of unknown pattern characteristics and the method for integrating determines the assumption of pattern shape in these regions.

One method of integration uses the coordinates ϕ and θ representing the antenna azimuth and elevation axes, as shown in Fig. 2. The basic rectangular differential area is also shown having the dimensions $r\,d\phi$ and $r\cos(\phi)\,d\phi$. The antenna power falling on this differential area is $P(\phi,\theta)$. This power level, as determined from the patterns, is a power density such that the power in the differential area, dP, is the power density times the area or

$$dP = P(\phi,\theta)\, r^2 \cos(\phi)\, d\phi\, d\theta \qquad (1)$$

The integration is indicated mathematically over the full sphere giving the total power radiated,

$$P_t = \int_{0}^{2\pi} \int_{-\pi/2}^{\pi/2} r^2\, P(\theta,\phi) \cos(\phi)\, d\phi\, d\theta \qquad (2)$$

The total power is later divided by the area of the sphere, $4\pi r^2$, to average the total power over the full sphere and obtain the power density that would be radiated by an omnidirectional radiator using the same value of total power. The r^2 term will cancel; therefore, it is given a value of unity for convenience.

The information available for use in this integration is the azimuth and elevation patterns which give $P(\theta)$ for $\phi = 0$ and $P(\phi)$ for $\theta = 0$. The information in 45° patterns would be difficult to handle by this method of integration. The resultant integral using only conventional azimuth, $P(\theta)$, and elevation, $P(\phi)$, patterns reduces to

$$P_t = \int_0^{2\pi} \int_{-\pi/2}^{\pi/2} P(\theta)\ P(\phi)\ \cos(\phi)\ d\phi\ d\theta \qquad (3)$$

This means that the pattern shape $P(\theta)$ is assumed to be the same for all values of ϕ and the pattern shape $P(\phi)$ is the same for all values of θ. Thus, the 3-dimensional pattern must necessarily take the general shape as shown in Fig. 3. Here it is observed that the pattern shape that must be assumed for this method of integration minimizes the extent of sidelobes in the quadrants between major axes.

In the second method of integration, the coordinates are chosen as shown in Fig. 4. The coordinate θ is the angular displacement from the antenna axis and α is the angular rotation around the antenna axis. This is co enient where there is circular symmetry. With coordinates chosen in this manner, the differential area is a rectangle of dimensions $r\ d\theta$ by $r \sin(\theta)\ d\alpha$ as shown in Fig. 4. Thus, as above, total power is given by

$$P_t = \int_0^{\pi} \int_0^{2\pi} r^2\ P(\theta,\alpha)\ \sin(\theta)\ d\alpha\ d\theta \qquad (4)$$

Again the term r^2 will ancel when determining power density per unit solid angle so that r is given the value of unity for convenience. The antenna pattern data, as mentioned above, is in the form of conventional single plane patterns, and assumptions must be made about the regions off axis. Patterns are not normally taken as a function of α but only in the θ coordinate. However, when the coordinate α is given the discrete values of 0°, 45°, 90°, and 135°, θ represents the azimuth, 45°, elevation, and 135° patterns respectively. The simplest and most accurate approach is to take the average of all half patterns giving a single averaged half pattern as shown in Fig. 5 of shape $P(\theta)$. Circular symmetry is assumed such that the average half pattern is independent of α and Eq. (4) reduces to

$$P_t = 2\pi \int_0^{\pi} P(\theta)\ \sin(\theta)\ d\theta \qquad (5)$$

This process of using a half pattern determined from the average of all half patterns has been carefully verified by the NRL Antenna Branch as an accurate means for determining antenna gain for circular aperture antennas. The resultant 3-dimensional pattern shape that is necessarily assumed by this method is indicated in Fig. 6. This gives a more realistic and conservative weight to the sidelobes.

The second integration method was used because it can more readily utilize information in other than major axis pattern and it more closely matches the expected circular symmetry of the antenna pattern. In addition, the conservative sidelobe assumption is preferred.

The patterns were read point by point and the integration was performed graphically using Simpson's rule. Some patterns were rechecked using planimeter integration of $P(\theta)\sin(\theta)$ with good agreement. The patterns used for integration were taken with a boresight tower 200 feet high and at a distance of 4900 feet. This is inside the $2D^2/\lambda$ distance of 9000 feet, and RCA focused the antenna to the boresight tower for pattern measurement. This is generally accepted practice for large antennas where it is not practical to locate a boresight tower outside the near zone, and patterns are essentailly identical to far-field patterns when focused to the far-field. It has been verified that accurate patterns can be obtained with boresight towers at ranges at least down to half the near zone limit providing the antenna is focused to the tower. In general, any errors would tend toward the conservative direction and would result in a lower gain figure and higher sidelobes than actually exist in the antenna.

As stated above, the total power P_t is divided by the total solid angle of 4π steradians to obtain the power density that would be radiated by an omnidirection antenna with the same total power. The gain G is the ratio of the power at the peak of the antenna pattern to the power density that would have been radiated by the omnidirectional antenna or

$$G = \frac{P_p}{P_t / 4\pi} \tag{6}$$

where: G is the power gain, and

P_p is the peak power of the main beam.

The far-out sidelobes, from spillover around the hyperbola, are determined by integration of feed patterns rather than integrating the sidelobes themselves. Figure 7 shows that the spillover sidelobes and the feed sidelobes (including part of the feed main lobe) are the same since with a Cassegrainian system the source is viewed directly by the feed (rather than by reflection from the hyperbola and parabola), at angles beyond that subtended by the Cassegrainian hyperbolic reflector. Figure 7 also shows that when the spillover sidelobes and feed sidelobes are plotted to be equal in amplitude on the same graph, the difference between the peaks of the antenna and feed patterns will be equal to the difference in gains of the feed and the antenna. The hyperbola and parabola simply use the feed energy subtended by the hyperbola ($\pm 18^\circ$) as shown in Fig. 7 and concentrate it into the narrow main beam of the antenna.

The spillover around the hyperbola was obtained by first integrating the feed patterns over the angle subtended by the hyperbola to obtain useful power and then using feed gain measurement to obtain total power. The percentage spillover loss is given by

$$L_s = 100 \frac{(P_t - P_h)}{P_t} \tag{7}$$

where: P_t is the total power radiated by the feed,

P_h is the useful power falling on the hyperbola, and

L_s is the percentage loss.

The useful power, P_h, which illuminates the hyperbola, was determined by integrating the feed patterns over the $\pm 18^\circ$ solid angle subtended by the hyperbola. The 45° patterns are also included for maximum accuracy. The same integration method was used as for the antenna pattern integration to obtain P_h from the feed patterns with point by point graphical integrations out to the $\pm 18^\circ$ angle subtended by the hyperbola.

Total power P_t is difficult to obtain accurately by pattern integration; therefore, a technique was used where gain is measured and P_t

determined from Eq. (6). Gain of the feed can be easily and accurately measured because the feed gain is about the same as that for the gain standard horn; thus, providing high accuracy for the value of P_t.

Solving for P_t in Eq. (6) gives a resultant which is a function of the main lobe P_p. However, useful power, P_h, as determined by pattern integration, is composed of a constant multiplied by P_p. Therefore, P_p may be given a nominal value of unity both for determining P_t with Eq. (6) and as an assumed peak pattern value when integrating to obtain P_h. The values of spillover loss determined by this technique are given in Table I.

The microwave comparator plumbing could not be conveniently removed from the feed, so that the plumbing loss decreased the value of gain measured from actual feed gain. Therefore, the measured values of gain are increased, as indicated in Table I, by the amount of the comparator loss, measured by RCA, because this loss should not be charged to antenna gain but to transmitter and receiver plumbing loss. The feed gains measured were between 15.4-db and 16.8-db. Each value of measured gain was increased by the amount of the comparator loss. This loss measurement is described in detail in an RCA letter to NASC MJ-462-FXL-975 of 6 November 1963. The values varied from about 0.3-db at 5400 Mc. to about 0.2-db at 5900 Mc.

The separate determination of spillover loss was helpful in showing some important characteristics of the antenna; and, in particular, the reason for a major source of loss being considerably higher than expected. In the original design consideration, about 32% spillover around the hyperbola was expected; however, by integration techniques it was found to be about 53% resulting in about 1.5-db greater than predicted loss.

The excess spillover loss is caused by two factors. First, the five horn feed configuration restricts the sum horn to a smaller than optimum size. This is a compromise which is necessary to obtain a good circular polarization capability with a minimum complexity afforded by the state-of-the-art. The second factor that increased spillover loss was the septums used in the horn. The septums were used to provide a more nearly optimum taper in illumination of the parabola. This reduces the major sidelobes of the antenna but causes very large feed pattern sidelobes. These sidelobes of

the horn feed are typically 7-db down from the feed pattern peak and appear as the large far-out sidelobes of the antenna as demonstrated by Fig. 7.

It was not certain what effect septum removal would have on the major sidelobes, but as a result of an arcing problem caused by the sharp edges of the septum tuning stubs, the septums and tuning stubs were removed in one radar. The major sidelobes did increase as expected but by one decibel. However, there were two main advantages observed. First, was an increase in antenna gain in the order of 1.7-db minimum over the band. The second advantage was a decrease in the large broad far-out sidelobe. With septums in the feed, the far-out sidelobes extended, at significant levels, from 18° to 80° with an amplitude of only 40-db to 50-db below the main lobe while removal of the septums reduced the lobe to only an 18° to 30° extent. A major problem with the large far-out sidelobes is susceptibility to interference from radiation from other radars and electronic equipment. Thus, the septum removal significantly reduced MIPIR susceptibility to undesired radiation in addition to increasing gain.

Another large sidelobe causing susceptibility to undesired radiation was found on only one side of the main lobe and only in elevation patterns. This sidelobe peaked at only 30-db down from the main lobe, and was found to be caused by the spars supporting the hyperbola, so that it appeared in only those pattern cuts which are in the plane of a spar. There was some concern that the spar sidelobes may represent a significant loss; however, it was determined from patterns taken by RCA at various angles near zero elevation that this lobe was narrow in the direction cross-wise to the plane of the patterns where they are observed. (This data was reported in RCA letter to NASC MJ-462-FXL-899 of 12 September 1963.) RCA also performed experiments showing that the spar sidelobe can be reduced by absorbent material. However, RCA found that most of the energy in this sidelobe comes from the far-out spillover sidelobes Thus, with the reduced spillover by septum removal, the spar sidelobes drop to a level which should not give significant susceptibility to undesired radiation.

Other losses are small and only estimated values are used since even a large percentage error will not significantly affect the value of overall gain. These values are indicated in Table I. The patterns are also carefully examined for any indication of significant deviation from normal values of these losses.

Table II gives the values of basic gain and actual gain, including all losses, for several antennas. It was agreed that NRL would analyze only one antenna and check others by pattern comparison. Antenna Serial No. 3 was analyzed at all three frequencies to establish the value of gain for acceptance. Where data was available on other antennas they were spot checked at 5400 Mc. as indicated in Table II. As indicated above, no feeds without septums were available for analysis. A figure of 1.7-db was chosen, as described above, as a reasonable figure to use on the basis of the expected increase in gain verified by the measurement of relative increase in gain.

A later evaluation of the AN/FPQ-6 radar at NASA Station, Wallops Island, Virginia* closely verified the results of the pattern integration technique, as shown in Table II, and the assumption of circular symmetry of the antenna patterns. Figure 8, is a contour plot and corresponding 3-D drawing prepared from data taken during the evaluation showing the high degree of circular symmetry in the main lobe and major sidelobe.

SUMMARY

Because of cost and accuracy limitations of various techniques considered for the AN/FPQ-6 radar antenna gain measurement, it was decided at an NRL, RCA and Air Force conference to use the antenna pattern integration method. This technique involved separate measurement of losses. As a result of this approach, several characteristics of the antenna were determined in addition to gain. This, in part, led to the removal of septums in the feed which, although increasing sidelobes about a decibel, increased antenna gain by about 1.7-db to the specified value of 51-db; thus, with septums removed the antenna meets its gain specification. The septum removal also greatly reduced the far-out sidelobes observed in the antenna pattern; thus reducing susceptibility to undesired radiation. High sidelobes caused by the spars were observed and techniques have been verified for effectively reducing them.

---

*R. Mitchell et al, "Final Report Measurements and Analysis of Performance of MIPIR, Missile Precision Instrumentation Radar Set AN/FPQ-6," by RCA Moorestown, N.J., under Navy Contract NOw-61-0428d, Dec. 1964.

The results of this gain determination, giving an average gain over the 5.4 to 5.9 gc band of 51.1-db, were later verified by an evaluation of the AN/FPQ-6 radar at NASA Station, Wallops Island, Virginia where measurements gave an average value over the band of 51.2-db.

ACKNOWLEDGMENTS

Mr. Russell Brown of the NRL Microwave Antenna and Components Branch provided considerable assistance and suggested some of the techniques used as in the feed spillover measurement.

Frequency Mc	Comparator Loss	Feed Gain (Compensated for Comparator Loss) db	Spillover Loss %	Spillover Loss db	Other Losses db	Total Losses db
5400	0.3	16.0	54	3.4	.5	3.9
5650	0.25	17.35	54	3.4	.5	3.9
5900	0.2	17.1	54	3.4	.5	3.9

(a) Feed spillover with a tabulation of total loss

Listing of Other Losses		
Type	%	db
Blockage	3	0.14
Tolerance effects	0.8	0.03
Depolarization	Negligible	
Spillover (around parabola)		0.34
Total		0.51db

(b) Other Losses

TABLE I - Data for Feed Spillover Loss for the Septimized Horn Only and Assumed Values for Other Losses.

Antenna	Frequency	Basic Gain db	Gain After Accounting For Losses		NASA Station Wallops Island Evaluation Dec. 1964 (Without Septums)
			With Septums db	Without Septums db	
Serial No. 3	5400 Mc.	53.2	49.3	51.0	50.5
	5650 Mc.	53.3	49.4	51.1	50.5
	5900 Mc.	53.4	49.5	51.2	52.7
Serial No. 1	5650 Mc.	53.3	49.4	51.1	
Serial No. 2	5400 Mc.	53.3	49.4	51.1	
Serial No. 5	5400 Mc.	53.2	49.3	51.0	

TABLE II - Antenna Gain Tabulation

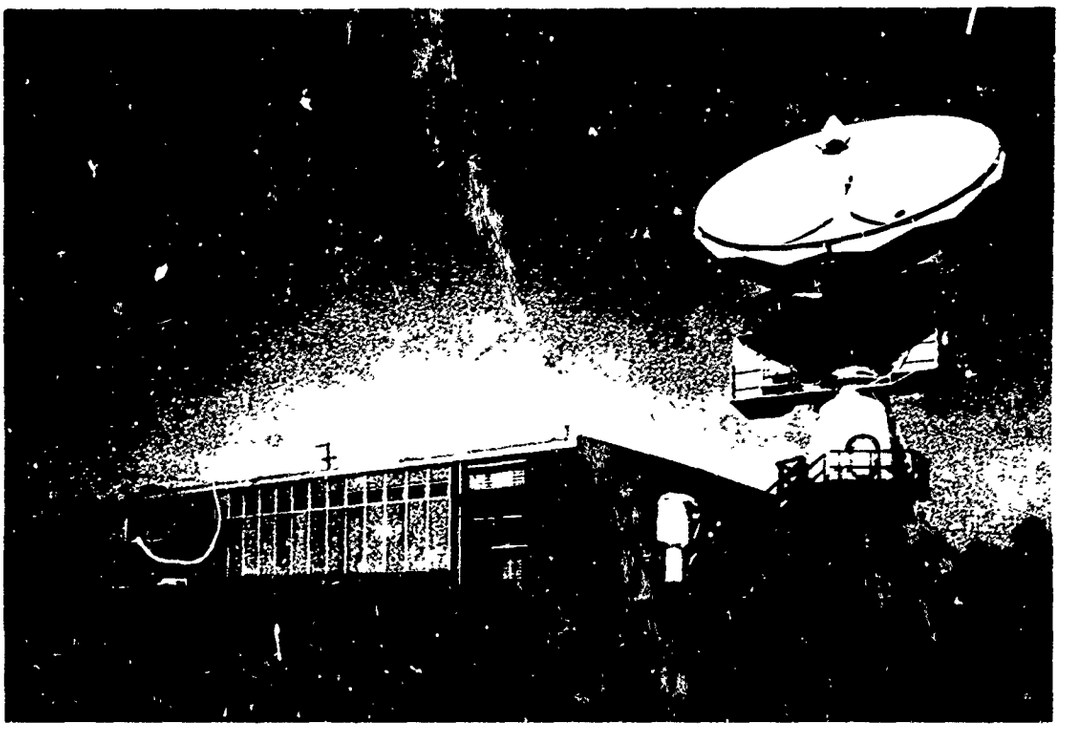

Fig. 1 - AN/FPQ-6 precision instrumentation radar installed at NASA Station, Wallops Island, Virginia

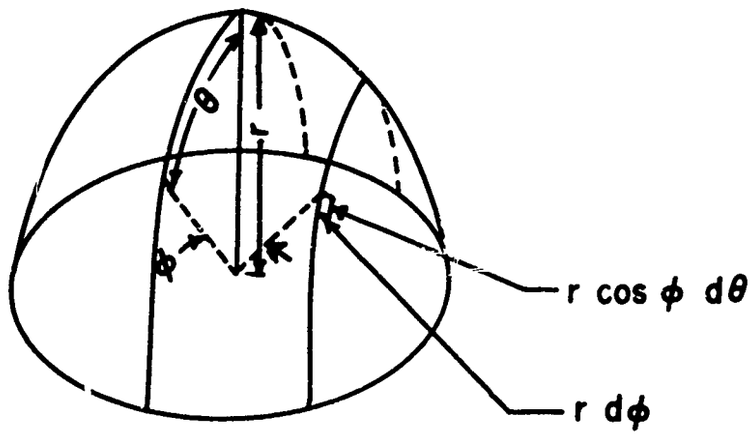

Fig. 2 - Diagram of the θ, ϕ coordinate system

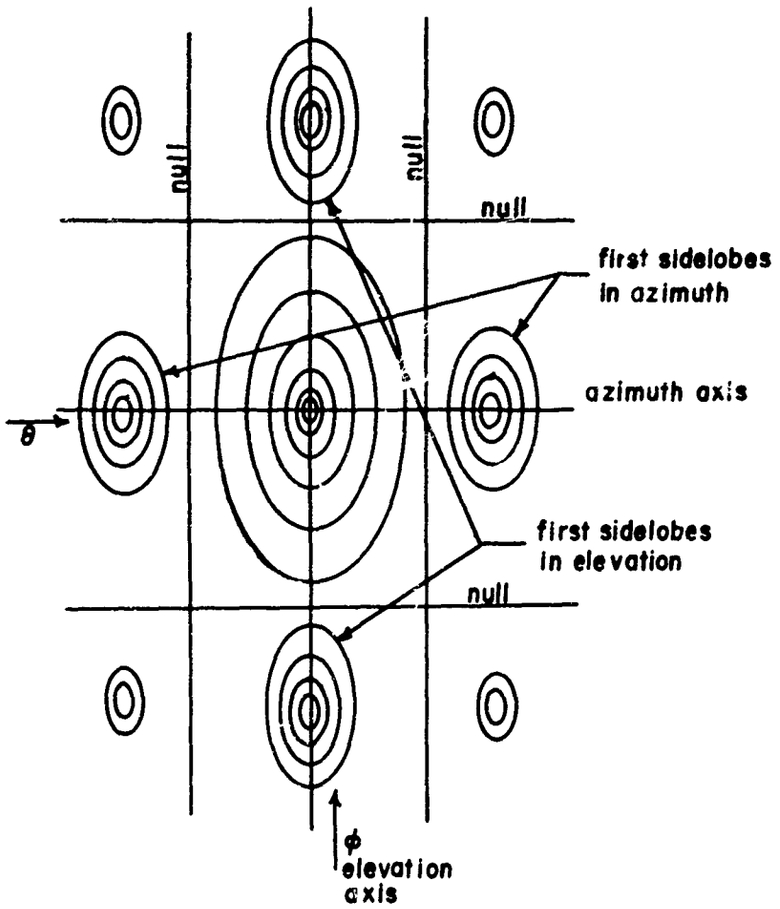

Fig. 3 - Three dimensional pattern shape assumed when using θ, ϕ coordinates

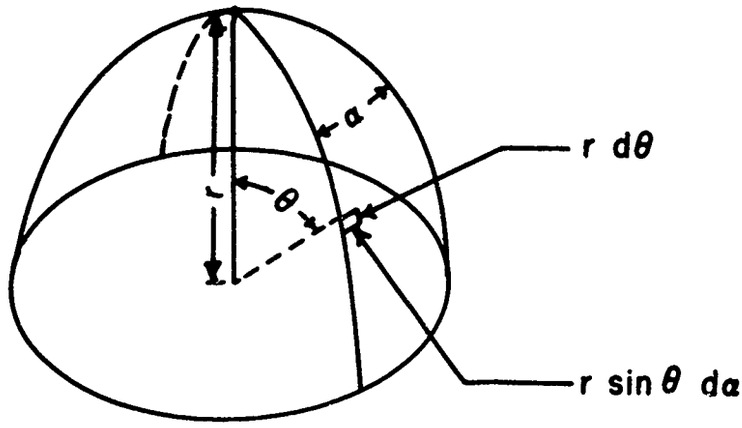

Fig. 4 - Diagram of the θ,α coordinate system

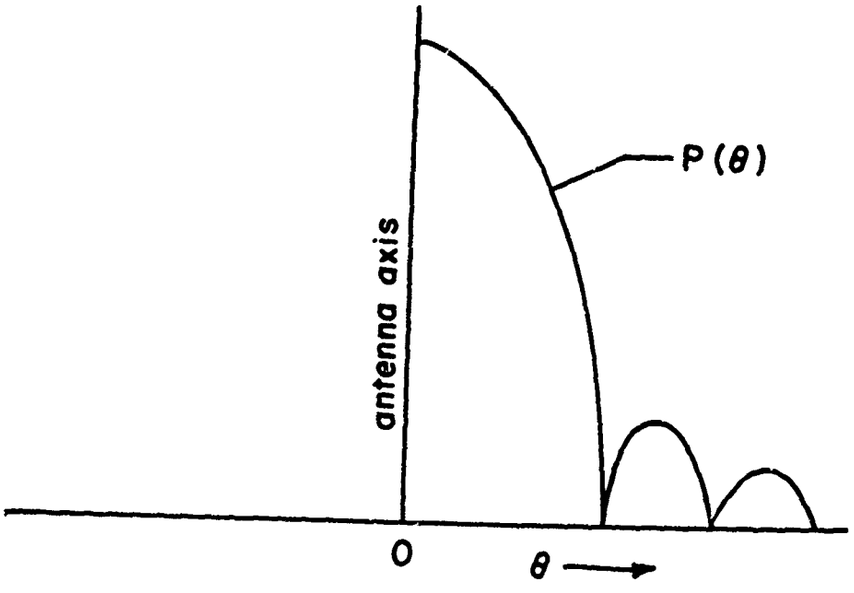

Fig. 5 - Half pattern average of all patterns

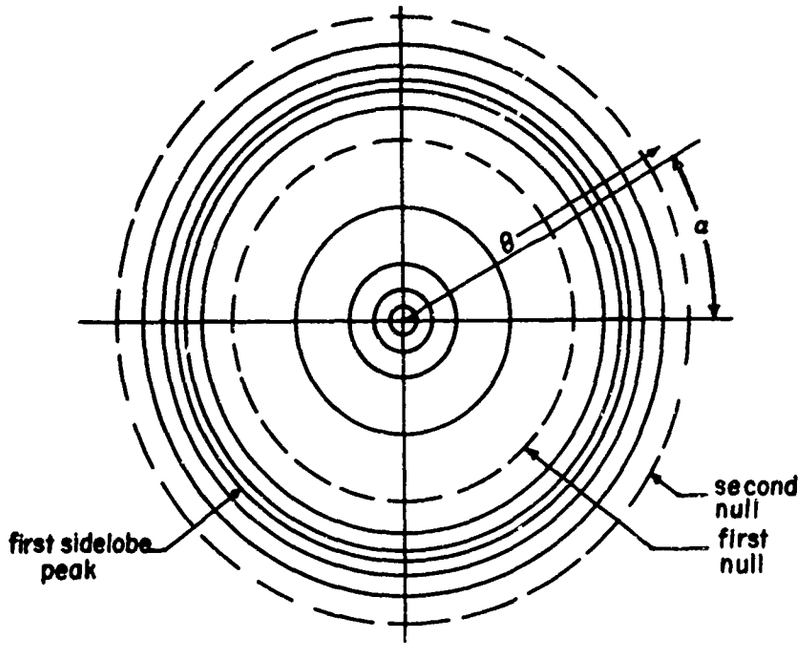

Fig. 6 - Three dimensional pattern shape assumed when using θ, α coordinates

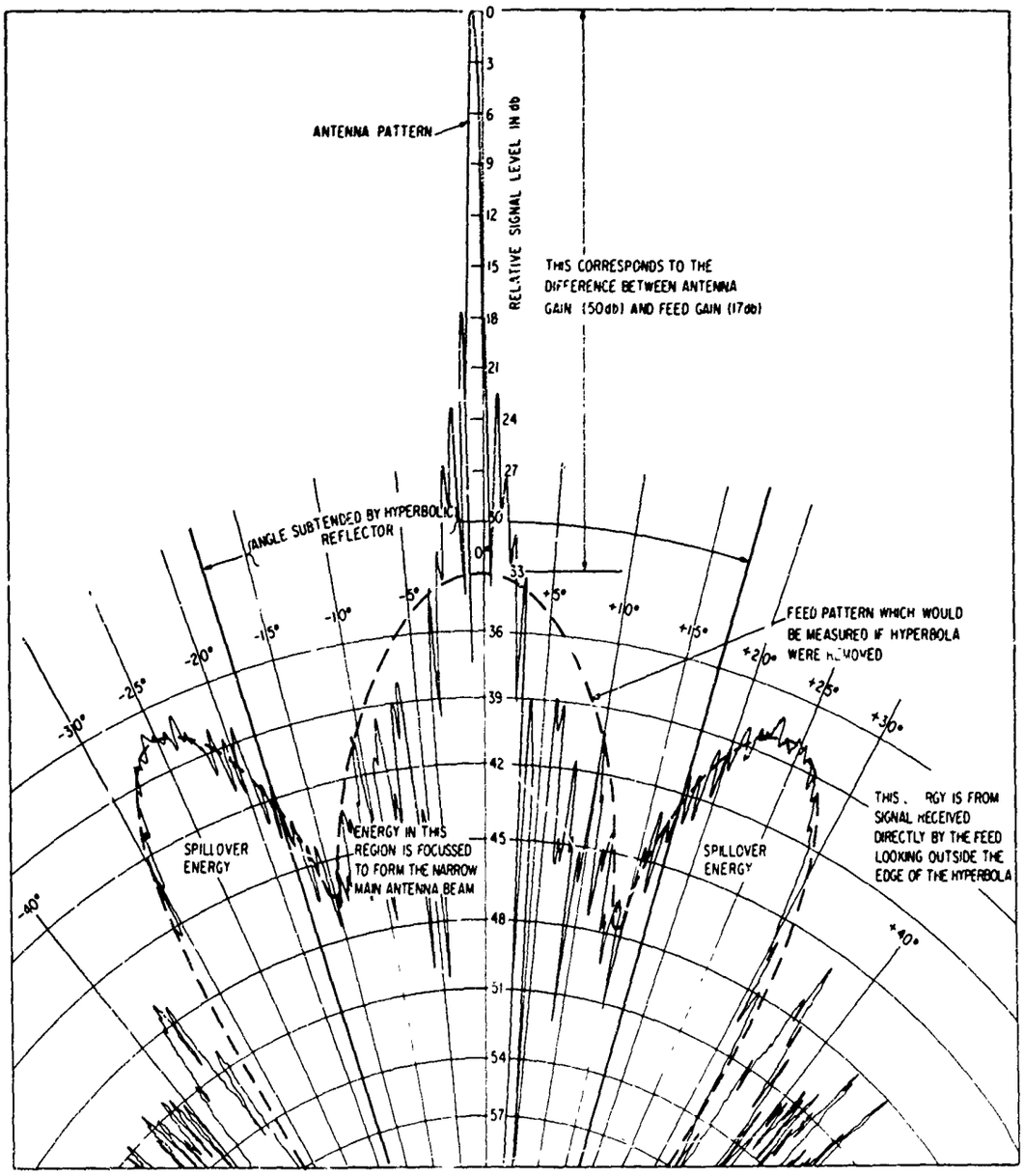

Fig. 7 - Antenna pattern with feed pattern superimposed to show the relation of spillover lobes in the antenna pattern to feed sidelobes

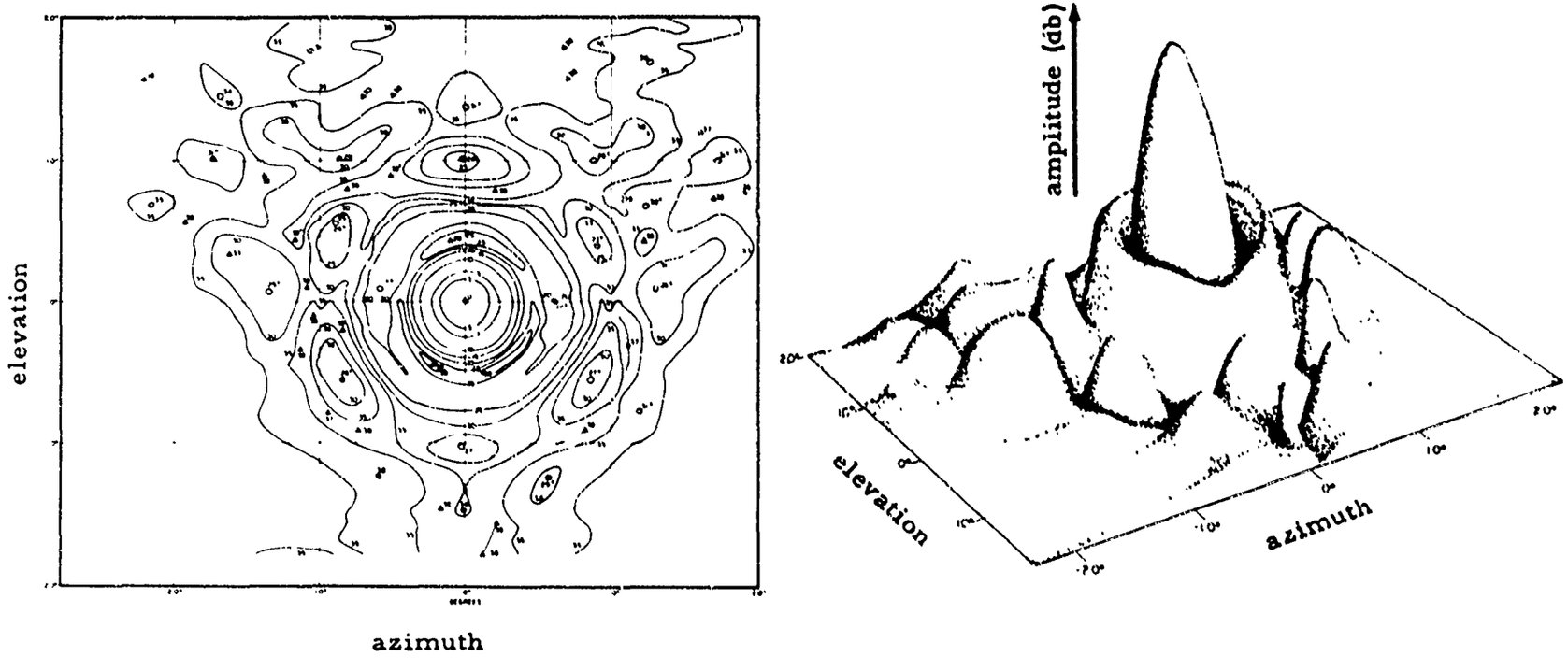

Fig. 8 - Contour pattern, (a) plot of equal amplitude contours of the main lobe and near-in sidelobes of the ANLFPQ-6 radar antenna where the numbers for each contour are db below the main lobe peak and (b) three-dimensional drawing of the antenna contour plot where height represents amplitude with a db scale.

Security Classification

DOCUMENT CONTROL DATA - R & D

(Security classification of title, body of abstract and indexing annotation must be entered when the overall report is classified)

ORIGINATING ACTIVITY (Corporate author) Naval Research Laboratory Washington, D. C. 20390	2a. REPORT SECURITY CLASSIFICATION Unclassified 2b. GROUP

3. REPORT TITLE

AN/FPQ-6 RADAR ANTENNA GAIN DETERMINATION BY PATTERN INTEGRATION TECHNIQUES

4. DESCRIPTIVE NOTES (Type of report and inclusive dates)

Interim report on the problem

5. AUTHOR(S) (First name, middle initial, last name)

Dean D. Howard

6. REPORT DATE	7a. TOTAL NO. OF PAGES	7b. NO. OF REFS
June 23, 1967	24	1

8a. CONTRACT OR GRANT NO	9a. ORIGINATOR'S REPORT NUMBER(S)
NRL Problem R02-24 b. PROJECT NO A05-535-208/652-1/F099-0502 c. d.	NRL Memorandum Report 1784 9b. OTHER REPORT NO(S) (Any other numbers that may be assigned this report)

10. DISTRIBUTION STATEMENT

Distribution of this document is unlimited

11. SUPPLEMENTARY NOTES	12. SPONSORING MILITARY ACTIVITY
	Naval Air Systems Command Washington, D. C.

13. ABSTRACT

The acceptance test gain determination for the 29 foot diameter Cassegrainian antenna of the AN/FPQ-6 radar was performed by antenna pattern integration techniques. This approach was used because of time limitations and difficulties of setting up an accurate boresight range for conventional gain comparison with a gain standard. By pattern integration of both the antenna and the feed patterns, the effective loss of near-in sidelobes and the spillover around the Cassegrainian subreflector could be determined separately with good accuracy. This approach gives considerable information on several characteristics of the antenna which led, in part, to changes for improving antenna performance. The less significant losses were estimated. The resultant gain determined by this technique averaged at 51.1-db over the band. This was confirmed at a later evaluation program where direct measurement gave an average gain of 51.2-db over the band.

DD FORM 1 NOV 68 1473 (PAGE 1)

S/N 0101-807-6801

Security Classification

Security Classification

14 KEY WORDS	LINK A		LINK B		LINK C	
	ROLE	WT	ROLE	WT	ROLE	WT
Radar antenna AN/FPQ-6 Antenna gain determination Antenna pattern integration techniques Cassegrainian antenna						

DD FORM 1 NOV 68 1473 (BACK)
(PAGE 2)

Security Classification